Proceedings of the 2020 Bath/ASME Symposium
on Fluid Power and Motion Control
FPMC2020
September 9-11, 2020, University of Bath, Bath, United Kingdom

FPMC2020-2712

EXPERIMENTAL INVESTIGATION OF A HYDROSTATIC BEARING BETWEEN BARRELS AND PORT PLATES IN FLOATING CUP AXIAL PISTON PUMPS

Peter Achten, Robin Mommers, Jeroen Potma, Jasper Achten
INNAS BV
Breda, the Netherlands

ABSTRACT

Hydrostatic machines often have multiple hydrodynamic bearing interfaces, which also serve as a sealing interface. In axial piston machines, the bearing and sealing interface between the barrel and the port plate is a well known example. At reasonably high operating speeds, hydrodynamic effects create an oil film between the barrel and the port plate. This oil film will then, to a certain extend, lift the barrel from the port plate, thereby avoiding metal-to-metal contact.

The disadvantage of hydrodynamic bearings is, that they need a relatively high velocity of the sliding components, in order to reduce the friction. Below a certain speed, mixed lubrication and finally solid friction will occur. This results in strongly increased friction losses and wear.

Low speed operation has always been of interest for hydrostatic motors, which are often operated at close to zero speed or at low rotational speeds. But low and near zero speed operation has also become of importance for pumps when being operated in electro-hydraulic actuators (EHAs). Many of the existing pump principles are not allowed to be operated below a certain minimum speed, due to excessive wear which results from coulomb friction conditions. Furthermore, the stick-slip-behaviour creates additional nonlinear behaviour of the EHA-operation, and makes it difficult to control EHAs.

In order to overcome the disadvantages of hydrodynamic bearings, a new hydrostatic bearing has been developed [1]. In the new bearing, the sealing land of the barrel is divided into three concentric rings. In the middle ring, so called pockets are created. Each pocket has a direct connection with the corresponding port by means of a small groove. The new bearing not only lifts the barrel to a certain height, but also helps to counteract the tilting torque of the barrel.

The size of the pocket grooves determines the height of the oil film, and therefore also the leakage and viscous friction of the bearing and sealing interface. In a recent research project, INNAS has performed a number of experiments to measure the influence of the groove size on the overall efficiency, as well as on the leakage and torque loss. Measurements have been performed on a 24 cc floating cup pump in a speed range between 500 and 4000 rpm and a pressure range between 100 and 400 bar. At the end of the project, the range has been extended to a speed range between 0.23 and 4400 rpm, and a pressure range between 50 and 450 bar.

This paper describes some of the results of these experiments. The measured width of the pocket grooves is taken as a characteristic parameter for the size of the flow area and resistance of the pocket grooves.

Keywords: floating cup pump, tribology, hydrostatic bearing.

NOMENCLATURE

h	gap height
M	torque
n	rotational speed
p_1	supply pressure
p_2	pump pressure
p_3	case pressure
Q	flow
R_1	flow resistance of the first sealing land
R_2	flow resistance of the second sealing land
R_{groove}	flow resistance of the pocket groove
W	groove width

INTRODUCTION

One of the most important tribological interfaces in axial piston machines is between the rotating cylinder block or barrel, and the stationary port plate or valve plate. This interface is a combination of a face seal and a thrust bearing.

Sealing lands around the barrel ports prevent excessive volumetric losses, while, simultaneously, the sealing land creates a pressure field that helps to counteract the force and torque loads acting on the barrel. These loads are not only pressure dependent, but also dependent on the rotational speed [2-5]. The design of this interface is furthermore complicated due to elasto-hydrodynamic effects [6, 7]. Also thermal expansion can deform the sealing areas, and can thus have an effect on the bearing capacity. In addition the varying pressure and oil temperature will strongly influence the viscosity of the oil, while passing the sealing areas [8-11].

In 2010, INNAS introduced a new design of the sealing lands [1]. Figure 1 compares a traditional design of the sealing land, and the modified new construction. Figure 2 shows a detailed picture of the new sealing land design.

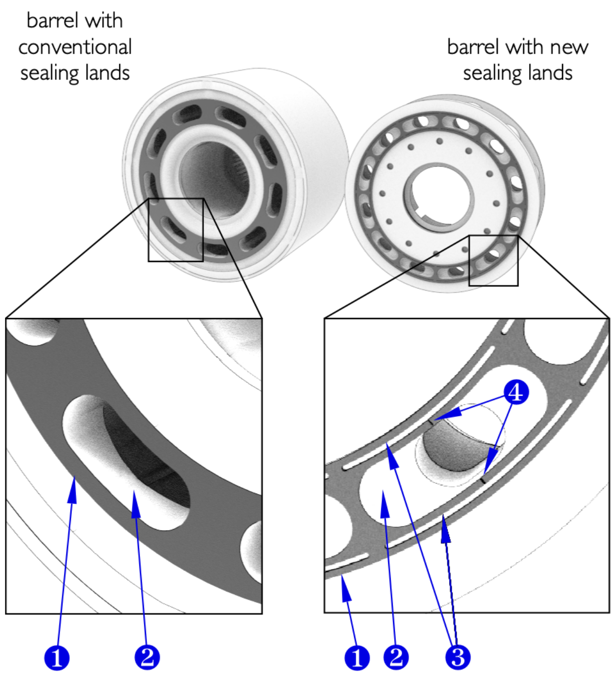

Fig. 1: Conventional sealing lands of a slipper type pump (left) and a barrel of a floating cup pump (right) with the new design of the sealing lands:

1. sealing land
2. barrel port
3. pockets
4. pocket grooves

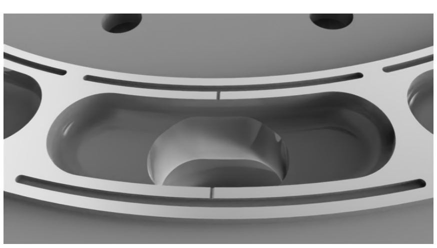

Fig. 2: Detailed view of a single barrel port with pockets on both sides of the port

The new design divides the sealing land in two separate sealing lands, split by a recessed area (the pocket). Each pocket is connected to the corresponding barrel port by means of a tiny groove. Figures 1 and 2 show a design with pockets on both the inner and the outer sealing land. It is, however, also possible to only have a pocket on the inner or outer sealing land.

The pressure level in the pocket is dependent on several leakage paths. Oil will flow from the barrel port to the pocket, via the pocket groove and via the first sealing land. This supply of oil will increase the pressure in the pocket.

In addition, oil will leak from the pocket to the case through the gap of the second sealing land. This flow of oil will reduce the pressure in the pocket. The oil supply via the first sealing land and the groove will be balanced with the oil leaking via the second sealing land, and create a balance pressure in the pocket.

The oil flow via the sealing lands is strongly dependent on the gap height, whereas the flow through the pocket grooves is nearly independent of the height of the gap between the barrel and the port plate. However, the flow through the grooves will strongly affect the pocket pressure and thus the gap height between the barrel and the port plate.

The pocket bearing design has a number of advantages. The pockets lift the barrel and prevent metal-to-metal contact, even at low or close to zero rotational speeds. Instead of being only a hydrodynamic bearing, the interface between the barrel and the port plate has now also become a hydrostatic bearing. The grooves are open on one side, which avoids clogging of the grooves, despite their small size.

In order to investigate the effects of the groove dimensions on the pump performance, INNAS has conducted a number of tests, in which the size of the pocket grooves has been reduced step by step. The tests are performed on a 24 cc floating cup pump, in a large speed and pressure range. The efficiency and the torque losses have been measured using a methodology described in [12]. In addition the case drain flow has been measured.

EFFECT OF THE POCKET GROOVES

Due to leakage, the pressure level will drop in the radial direction of the sealing lands, being equal to the pump pressure p_2 at the start of the leakage path, and equal to the case pressure p_3 at the end of the leakage path. With the pockets, the pressure profile will have a plateau at pressure p_{pocket}. Three resistances have a major effect on the pocket pressure (see Figure 3):

- Resistance R_1 of the first sealing land between the barrel port and the pocket;
- Resistance R_2 of the second sealing land between the pocket and the pump case
- Resistance R_{groove} of the pocket groove

Resistance R_1 and R_2 are strongly dependent on the gap height, and can therefore be considered as variable resistances. The third resistance R_{groove} is nearly independent on the gap height between the barrel and the port plate. The system acts like a pressure divider. At small gap heights h, R_1 and R_2 will become much higher than R_{groove}. Since at $h \approx 0$, and R_1 and R_2 being much larger than R_{groove}, the pockets will become filled with oil via the pocket groove. This creates a high average pressure level across the sealing land, thereby lifting the barrel from the port plate.

On the other hand, when the gap height increases too much, R_1 and R_2 can become much smaller than R_{groove}. In that case, the pocket pressure drops, which also results in a lower average pressure level across the sealing lands. This will reduce the gap height.

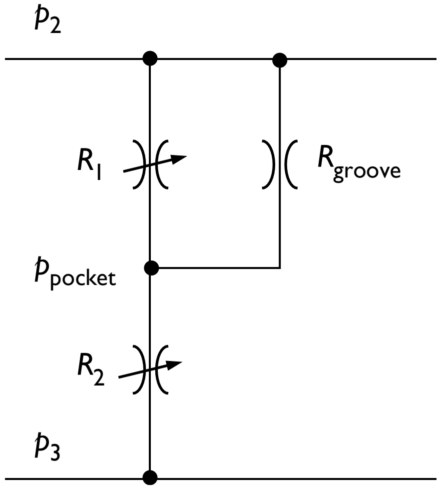

Fig. 3: Hydraulic circuit of a sealing land with a pocket, two sealing lands (R_1 and R_2) and a groove (R_{groove})

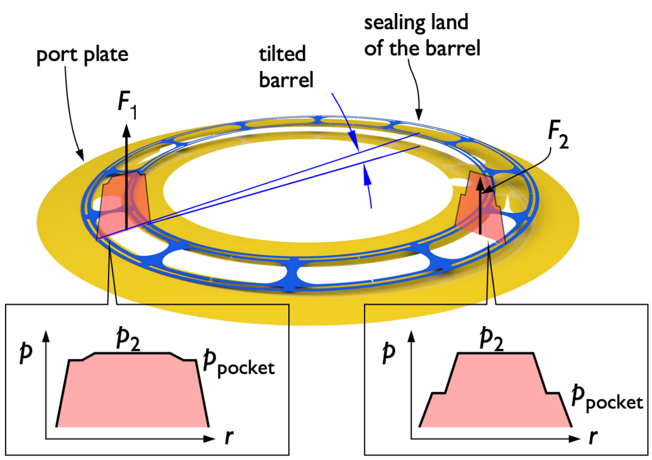

Fig. 4: Effects of a tilted barrel on top of the port plate. Only the sealing lands of the barrel (blue) and the top of the port plate (orange) are shown.

The pockets not only help to lift the barrel a few micrometer in the axial direction, but also counteract any tipping load on the barrel. This is illustrated in Figure 4, which shows only the surface of the port plate and the sealing lands of a slightly tilted barrel. The figure shows two pressure profiles of the sealing lands, one for the situation in which the barrel almost touches the port plate (the left profile), and one where the sealing land is at a rather large distance from the port plate. The first section of the sealing land will create a large lifting force, due to the high average pressure level of the sealing land. Now, the dimensions of the sealing lands can be chosen as such that the lifting axial force F_1 is larger than the hydrostatic force from the piston. In that case, the barrel will be lifted from the port plate. At a larger distance from the port plate, the sealing land force can become smaller than the piston force. If the barrel is tilted, as is shown in Fig. 4, forces like F_1 and F_2 will create a torque on the barrel, which will correct the tilted barrel position.

DEFINITION OF THE RESEARCH PROJECT

The pump being tested for this research project is a 24 cc fixed displacement, floating cup pump/motor, as is developed by INNAS (FCM24). The pump/motor is designed for 4-quadrant operation, and needs a supply pressure of 6 bar to avoid cavitation at the highest rotational speeds. It is not necessary to have pockets on each side of each barrel port. In this paper, the pump is tested with only pockets on the inner sealing land of the barrel (Figure 5). The FCM24 is tested at the test bench of Innas [13].

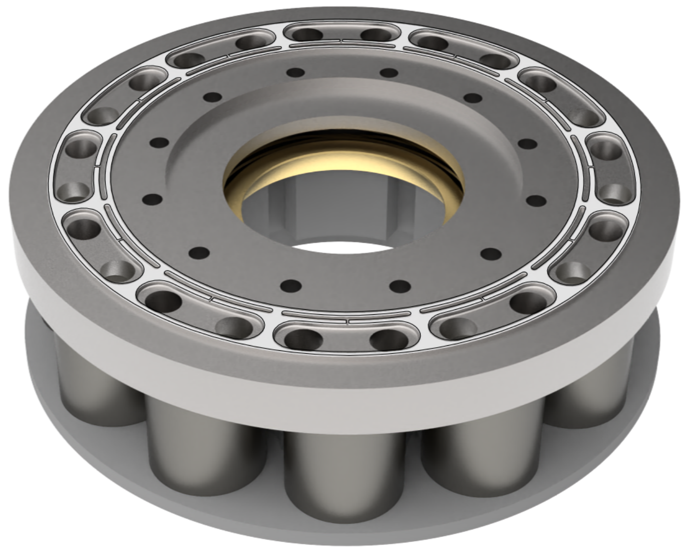

Fig. 5: Barrel with only having pockets in the inner sealing land

The objective of this study is to measure the effect of the groove dimensions i.e. the cross sectional area, on the overall efficiency, on the torque losses and on the case drain losses. The cross sectional area of the grooves is varied by lapping the sealing area (the white area in Figure 5) of the barrel, layer by layer.

In addition, the wear of the port plates will be monitored. It is expected that with the large grooves the barrel will lift to such an extend, that there will be no significant wear of the port plates. After each lapping step, the grooves will be reduced in size, and the gap height is expected to become smaller and smaller. The lapping procedure will stop when there is significant wear of the port plates.

MEASUREMENT OF THE POCKET GROOVES

For a small machine, like the 24 cc FCM24, the grooves have a width of 100 to 200 µm. The depth is about half the width. There are several ways of manufacturing these grooves: by means of a small milling cutter, by means of EDM, or by

means of a laser. Figure 6 shows a microscopic, 3D-measurement of a groove which was manufactured by a milling cutter. In this research, EDM-machined grooves are applied.

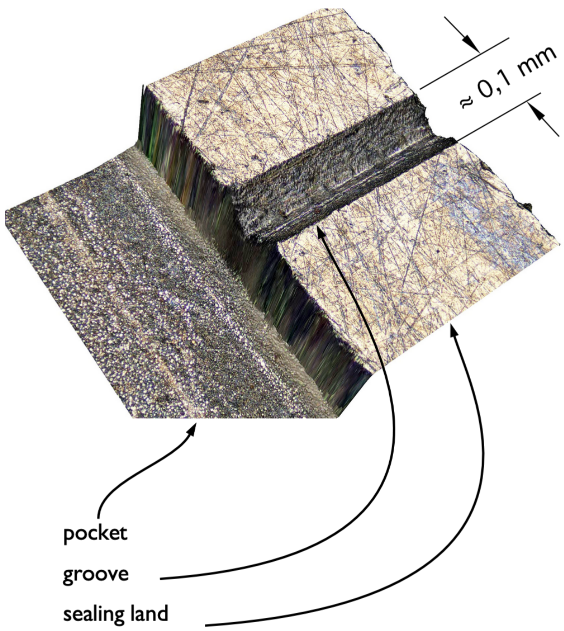

Fig. 6: Microscopic view of a pocket groove.

Considering that the barrel, with the V-shaped grooves, is running at a relatively high speed op top of the port plates, the flow through the groove is assumed to be turbulent. Consequently, the cross sectional opening area of the groove defines the flow resistance of the groove.

In this project, the width of the grooves is taken as a dimensional parameter for the flow area. The average width of each groove is measured by means of a 3D-microscope. This is repeated after every lapping procedure, which results in a step-by-step reduced cross sectional area of the grooves. Since there are two barrels in the pump, a total number of 24 grooves has been measured after each lapping procedure.

The two diagrams in Figure 7 show the results of these measurements. The measurements show that the grooves are not equal. In barrel 1, the fourth groove is for instance much smaller than the other grooves. Since this variation cannot be eliminated by lapping the sealing lands, and since the sealing lands need to remain flat across the entire area, the variation of the groove dimensions remain after each lapping step. Table 1 shows the average width of all grooves after each lapping procedure.

Table 1: Average groove width $\overline{W}$ of all grooves of both barrels after each lapping step

step	1	2	3	4	5	6	7	8	9
$\overline{W}$ [μm]	212	201	195	186	175	162	150	137	124

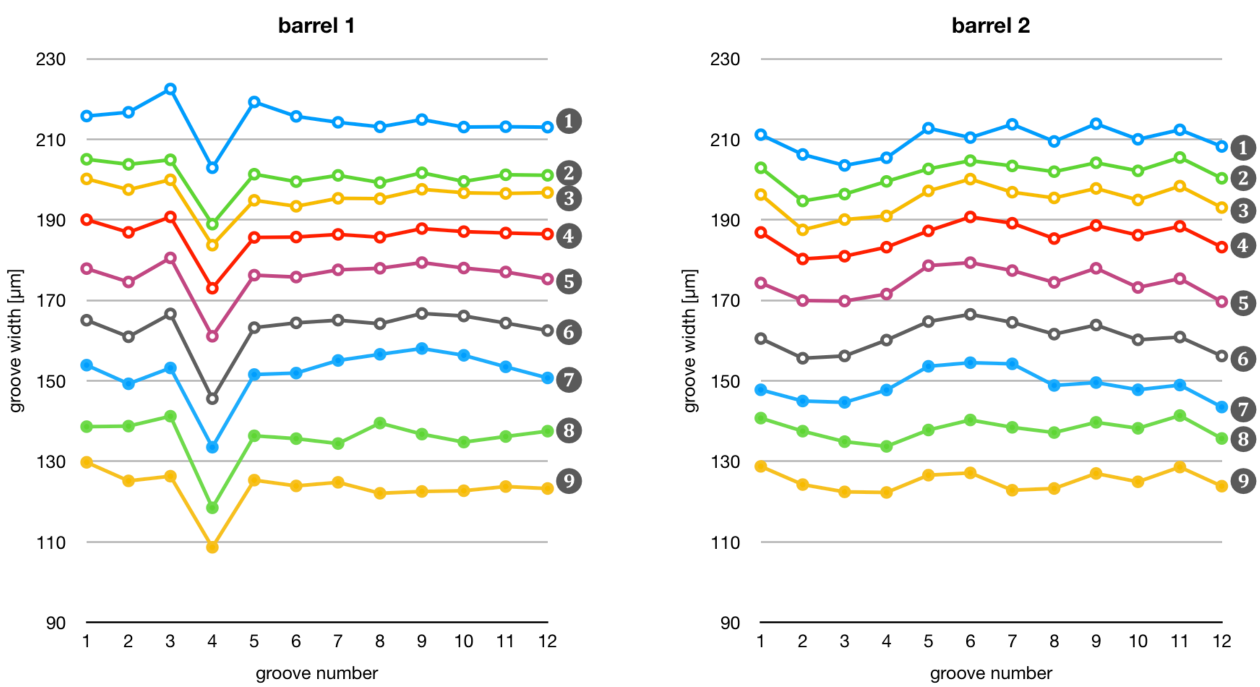

Fig. 7: Measured width of the pocket grooves after each lapping step of the barrels.The encircled numbers on the right of each line indicates the number of the lapping step by which the groove are made smaller.

PERFORMANCE MEASUREMENTS

After each lapping procedure, the pump was tested in a number of operating points. The rotational speed was varied between 500 and 4000 rpm, with 500 rpm increments; the pump pressure was varied between 100 and 400 bar with 100 bar increments. This results in 32 stationary operating points in which the performance of the pump has been measured. The barrels have been lapped 9 times to reduce the flow area of the groove, and after each lapping operation, a complete field of 32 points has been measured. More information about the test bench and the sensors being used can be found in [13]. The test results are evaluated using the methodology described in [12]. The oil temperature at the inlet is 50°C. The oil is Shell Tellus 46 (HLP 46). The supply pressure is 6 bar.

The first parameters to be evaluated are the overall efficiency, the case drain (leakage), and the overall torque losses. The overall torque loss is an addition of several dissipative and friction related losses:

1. Flow losses
2. Churning losses
3. Friction losses of the tapered roller bearings
4. Friction losses between the cups and the pistons
5. Friction losses between the cups and the barrels
6. Losses due to commutation
7. Friction losses between the barrels and the port plates

The first three losses have been measured and are known. Loss terms 4 and 5 have been measured as well and are negligible. The losses due to commutation are calculated by means of a simulation model of the pump. Having measured the overall torque loss, and knowing losses 1 to 6, the seventh loss term, the friction between the barrels and the port plates, can be calculated. This is important, since this is the term that is directly influenced by the groove dimensions.

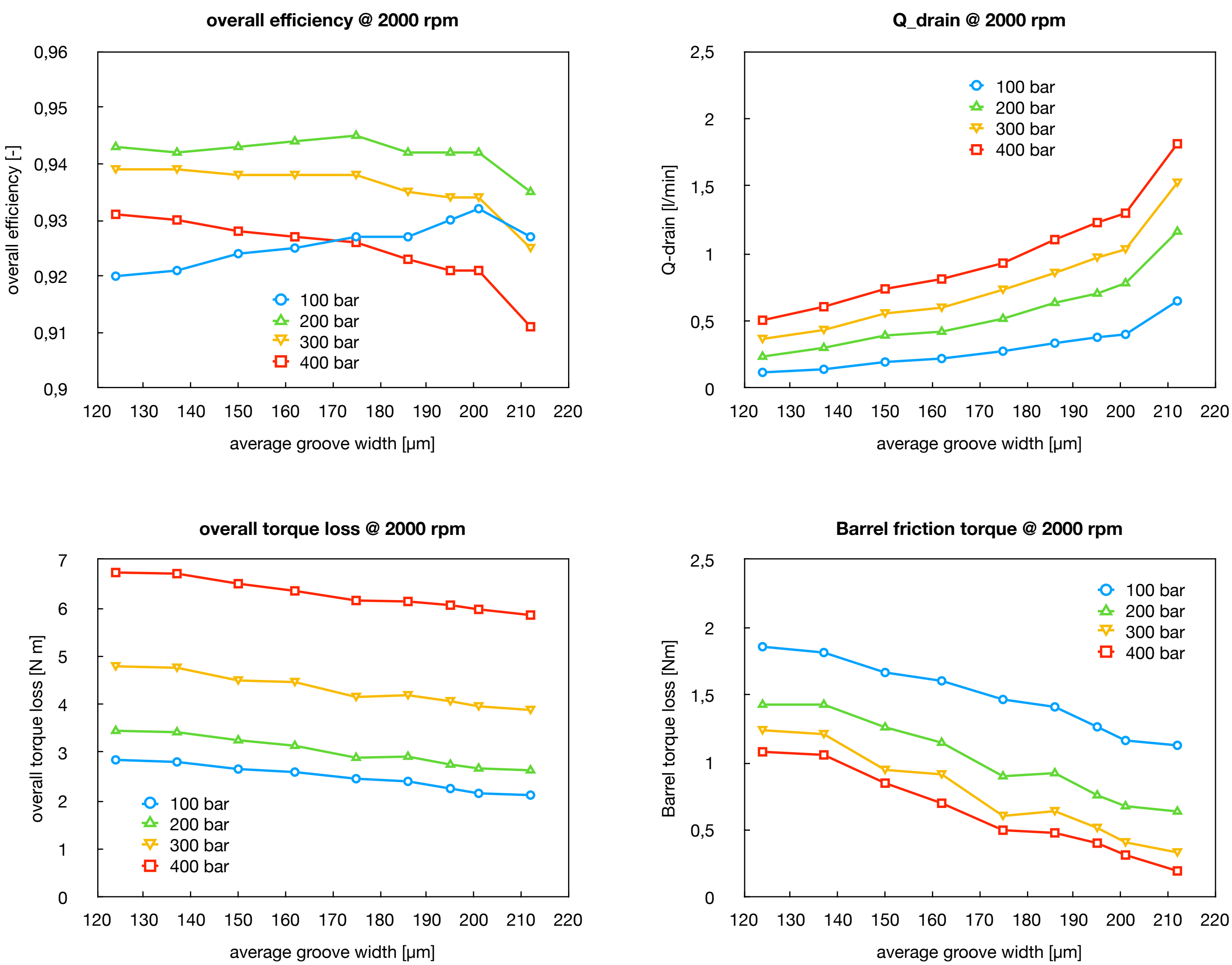

Fig. 8: Influence of the average groove width on the overall efficiency, the case drain flow, the overall torque loss, and the specific torque loss of the (two) barrels running on the port plates. The measurements are performed at stationary conditions at a rotational speed of 2000 rpm.

For a rotational speed of 2000 rpm, the results are shown in Figure 8. There are four diagrams:

- The overall efficiency
- The case drain
- The overall torque loss
- The specific torque loss of the barrels

All diagrams show the average groove width of both barrels as a parameter. Appendix A shows the results for other rotational speeds.

The measurements show that the effects of the groove width on the efficiency strongly depend on the pump pressure. Changing the groove width from 212 to 201 µm results in an improvement of the overall efficiency at all pressure levels. This is especially due to a strong reduction of the case drain losses.

Aside from this first step of a reduction of the groove width, the overall efficiency is hardly affected by the groove width for pump pressures of 200 and 300 bar. However, at 100 bar, the efficiency is reduced when the groove width is reduced below 201 µm. On the other hand, at 400 bar, the overall efficiency shows a significant and continuous improvement of the efficiency even at the smallest groove width of 124 µm.

A reduction of the flow area of the grooves increases the flow resistance of this groove. As a result, the pressure in the pockets is reduced which results in a smaller gap height between the barrel and the port plate.

The smaller gap height obviously results in a reduction of the leakage flow, as can be seen in the measured case drain losses. On the other hand, the smaller gap height increases the viscous losses, which explains the increased overall torque loss, as well as the specific torque loss between the barrels and the port plates. This effect is clearly visible in the diagrams showing the overall torque loss and the barrel torque loss. The last diagram also shows that the barrel torque loss is smaller for higher pressure levels. This is probably due to the stronger effect of the pocket pressure at higher pump pressures.

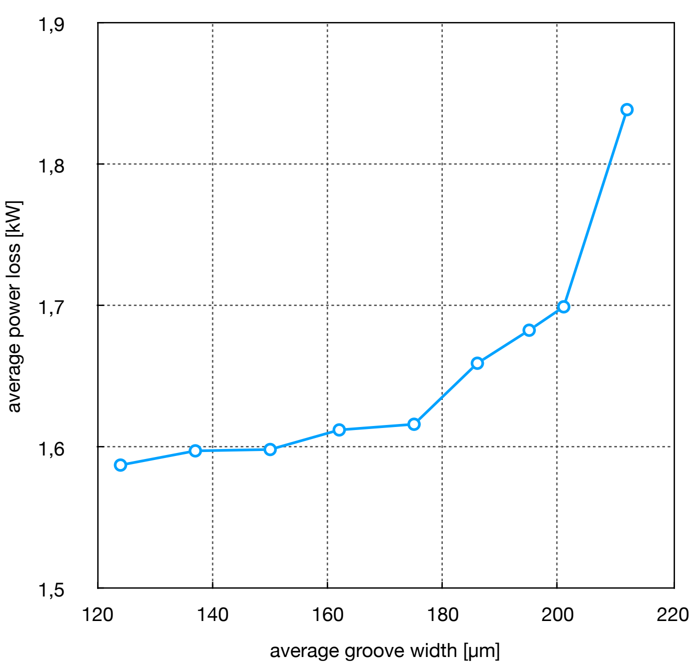

Fig. 9: Measured average power loss, all points of operation being weighted equally ($500 \leq n \leq 4000$ rpm, $100 \leq p_2 \leq 400$ bar).

Figure 9 shows the influence of the average groove width on the average value of the overall power losses. The average power loss is determined as the average value of the measured power losses in all points of operation between 500 and 4000 rpm and 100 and 400 bar. All points are weighted equally.

The diagram of Figure 9 shows, that a reduction of the groove width from 212 to 175 µm gives a significant reduction of the average power loss. After that, a further reduction only results in a small reduction of the average power loss. This is an indication for the precision with which the grooves have to be manufactured. Between 124 and 175 µm there is not a large effect of the groove width (and depth) on the average power loss. However, the groove width does still have a significant effect on the volumetric losses. The case drain flow is reduced by about 50% by means of reducing the groove width from 175 to 124 µm.

PORT PLATE WEAR

In the pump, the steel barrel is much harder than the brass port plate. Wear will therefore be seen on the latter component. After each lapping procedure and performance test, the port plates have been inspected and measured. Only after the last lapping step, one of the port plates (port plate 1, corresponding to barrel 1 of Figure 7) showed some beginning of abrasive wear. The other port plate (port plate 2) hardly showed any wear. The wear is characterised as circular grooves with a depth of up to 4 micrometer. This is the point where it was decided not to continue lapping the barrels and not to reduce the groove dimensions any further.

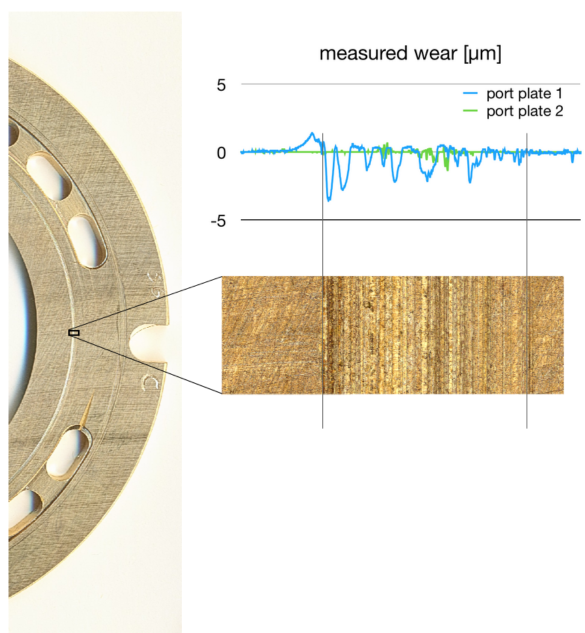

Fig. 10: Detailed wear measurement of the port plates

EXTENDED PERFORMANCE MEASUREMENTS

At the end of the project, the pump has been tested again for a much more extended range of operating conditions (Table 2). In this final test, the pump has been tested in 144 operating points. The range has especially been extended in the low speed range.

At low rotational speeds, the geometrical displacement of the pump is lower than the volumetric losses. In Table 2, these points are marked with a red colour. In the red points, the pump is not able to create the desired pressure level. Nevertheless, in order to be able to measure the torque losses and case drain losses in these points, an additional pump has been used to create the desired pressure. Effectively, in these red marked operating points, the overall efficiency of the pump has become zero or undefined. But the goal of the research project was also to see how effective the new bearing is as a hydrostatic bearing, i.e. also at low and very low operating conditions. And these parameters can still be measured, also when an additional pump is applied.

Table 2: Operating points for the final performance test. The points which are marked in red, an additional pump has been used to maintain the desired pressure level.

	pump pressure [bar]								
n [rpm]	50 bar	100 bar	150 bar	200 bar	250 bar	300 bar	350 bar	400 bar	450 bar
0.23	✓	✓	✓	✓	✓	✓	✓	✓	✓
0.93	✓	✓	✓	✓	✓	✓	✓	✓	✓
10	✓	✓	✓	✓	✓	✓	✓	✓	✓
25	✓	✓	✓	✓	✓	✓	✓	✓	✓
50	✓	✓	✓	✓	✓	✓	✓	✓	✓
100	✓	✓	✓	✓	✓	✓	✓	✓	✓
250	✓	✓	✓	✓	✓	✓	✓	✓	✓
500	✓	✓	✓	✓	✓	✓	✓	✓	✓
1000	✓	✓	✓	✓	✓	✓	✓	✓	✓
1500	✓	✓	✓	✓	✓	✓	✓	✓	✓
2000	✓	✓	✓	✓	✓	✓	✓	✓	✓
2500	✓	✓	✓	✓	✓	✓	✓	✓	✓
3000	✓	✓	✓	✓	✓	✓	✓	✓	✓
3500	✓	✓	✓	✓	✓	✓	✓	✓	✓
4000	✓	✓	✓	✓	✓	✓	✓	✓	✓
4400	✓	✓	✓	✓	✓	✓	✓	✓	✓

The four diagrams in Figure 11 show the results of these measurements:

- The overall efficiency (excluding the points marked in in Table 2);
- The case drain flow (i.e. overall leakage);
- The overall torque loss;
- The specific friction torque of both barrels (excluding the points marked in Table 2)

As mentioned before, the efficiency is no longer defined for points where the geometrical pump output is smaller than the leakage of the pump (the points marked in red). Furthermore, the analysis of the barrel torque loss is based on an energy balance, for which the measured overall power loss is required as a parameter. But, as for the overall efficiency, the overall power loss is not defined when an additional pump is used to maintain the desired pressure level. Therefore, these points are not shown in the diagrams of Figure 11.

The measurements show that the overall efficiency reaches a maximum above 96% when both the pump pressure and the rotational speed are low. Furthermore, the overall torque loss increases when the pump pressure is higher. This increase is mainly due to the higher commutation losses across the pressure relief grooves.

The case drain loss and the barrel friction torque loss are the most relevant for the function of the barrel sealing lands with the pockets and the pocket grooves. The analysis clearly shows how the friction losses of the barrels becomes smaller when the pressure level is increased. This is probably due to the fact that the effect of the pockets becomes larger when the pressure increases.

The measurements also show that the pocket-and-groove design realises a small friction torque loss between the barrels and the port plates, even when the rotational speed is reduced to below 1 rpm. There is only a mild increase of the friction loss at very low rotational speeds. This could be due to some light mixed lubrication, but most likely the temperature of the oil and the pump itself also influences the results. During the measurements, the oil temperature at the inlet is maintained at 50°C. But for very low speeds, the inlet temperature is not a measure for the oil temperature at the tribological interfaces. At low rotational speeds, the pump is no longer ‘cooled’ by means of the oil flowing through the pump. This strongly influences the barrel torque loss, but also the case drain flow.

CONCLUSIONS

A new hydrostatic bearing design for axial piston pumps and motors has been investigated empirically in a 24 cc, fixed displacement, floating cup pump. The main objective was to measure the effect of the size of the grooves feeding into the pockets which have been manufactured in the sealing lands. Only pockets at the inside diameter of the barrel ports have been applied; there are no pockets in the outer sealing lands. The width of the grooves has been used as a characteristic parameter for the cross sectional area and flow resistance of the grooves. The average groove width has been varied between 212 and 124 µm.

The groove dimensions have been changed by means of lapping of the sealing lands of the barrels. After each lapping step, the grooves have become less wide and less deep, which effectively increases the flow resistance of the grooves.

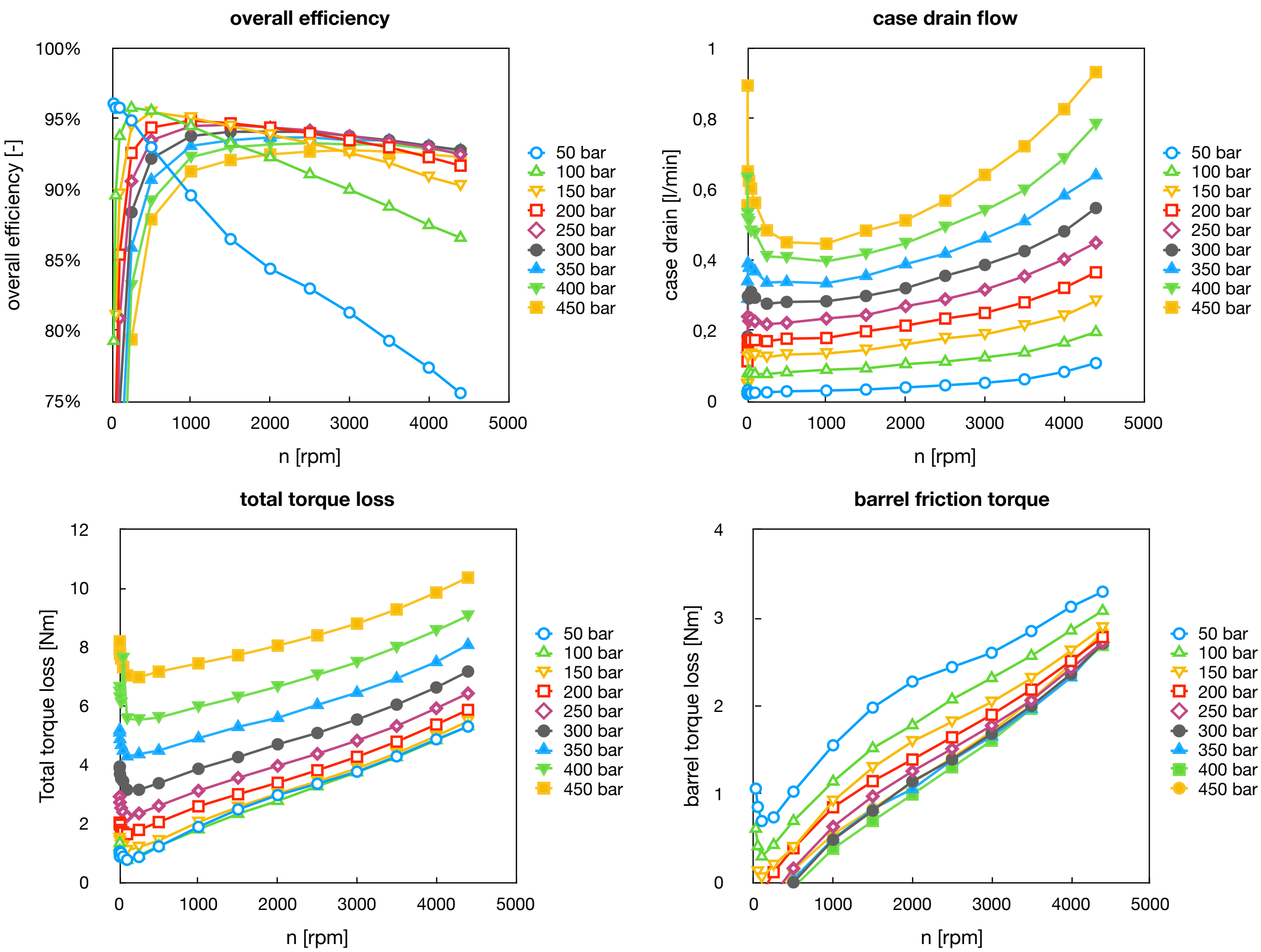

Fig. 11: Overall efficiency, case drain flow, total torque loss and the specific torque loss due to friction of the two barrels (average groove width = 124 µm)

The grooves have been reduced in nine steps. After each lapping procedure, the groove dimensions have been measured, and the performance of the pump has been measured in a range of operating speeds and pump pressures.

A reduction of the groove width and depth results in a reduction of the case drain flow and an increase of the barrel friction. The barrel friction is almost linearly dependent on the rotational speed of the barrel, indicating a viscous friction. The increased barrel friction for smaller grooves and the simultaneous reduction of the case drain both show that the average gap height is directly influenced by the groove dimensions.

The experiments have also shown that the application of pockets and grooves effectively eliminates any substantial wear of the barrel or the port plate, provided that the groove dimensions do not become too small.

Considering the overall efficiency, the groove do not need to be manufactured with a very high precision. A variation of the groove width between 124 and 175 µm resulted in almost the same average power loss.

REFERENCES

1. Achten, P.A.J., T.L.v.d. Brink, and G.E.M. Vael, *A robust hydrostatic thrust bearing for hydrostatic machines*. Proc. 7.IFK, March 22-24, 2010, Aachen, Germany, 2010: p. 100-112.
2. Manring, N., *Torque on the cylinder block of an axial-piston swash-plate type hydrostatic pump*. Retrospective Theses and Dissertations. Paper 11164, 1996.
3. Manring, N.D., *Tipping the Cylinder Block of an axial-piston swash-plate type hydrostatic machine.* Transactions of the ASME, 2000. 122: p. 216-221.
4. Manring, N.D., et al., *Scaling the Speed Limitations for Axial-Piston Swash-Plate Type Hydrostatic Machines*. Journal of Dynamic Systems, Measurement, and Control, 2014. 136(3): p. 031004.
5. Achten, P. and S. Eggenkamp, *Barrel tipping in axial piston pumps and motors*. Proc. 15th Scandinavion International Conference on Fluid Power SICFP17, June 7-9, 2017, 2017.
6. Achten, P.A.J. and M.P.A. Schellekens, *Deformation effects on the load carrying capacity of the barrel bearing in axial piston pumps and motors*. Proc. IMECE2006, 2006

ASME International Mechanical Engineering Congress and Expo November 5-10, 2006, Chicago, Illinois, USA, 2006.

7. Chacon, R. and M. Ivantysynova, *Thermal Effects on the Fluid Film in the Cylinder Block/Valve Plate Interface due to Compression and Expansion of the Fluid*. JFPS International Journal of Fluid Power System, 2019. 11(3): p. 136-142.
8. Pelosi, M., M. Zecchi, and M. Ivantysynova, *A fully coupled thermo-elastic model for the rotating kit of axial piston machines*, in Proc. Bath ASME Symposium on Fluid Power and Motion Control FPMC. 2010. p. 217 - 234.
9. Zecchi, M., *A novel fluid structure interaction and thermal model to predict the cylinder block:valve plate interface performance in swash plate type axial piston machines*. Dissertation Purdue University, 2013.
10. Li, Y., et al., *Thermal-fluid-structure coupling analysis for valve plate friction pair of axial piston pump in electrohydrostatic actuator (EHA) of aircraft*. Applied Mathematical Modelling, 2017. 47: p. 839-858.
11. Ji, Z., *Research on thermal-fluid-structure coupling of valve plate pair in an axial piston pump with high pressure and high speed*. Industrial Lubrication and Tribology, 2018. 70(6): p. 1137-1144.
12. Achten, P., et al., *Measuring the losses of Hydrostatic Pumps and Motors – A Critical Review of ISO4409 2007*, in ASME/Bath 2019 Symposium on Fluid Power and Motion Control FPMC2019. 2019: Sarasota, FL, USA.
13. Achten, P., J. Potma, and S. Eggenkamp. *A New Hydraulic Pump and Motor Test Bench for Extremely Low Operating Speeds*. in ASME/BATH 2017 Symposium on Fluid Power and Motion Control. 2017. Sarasota, Florida, USA.

APPENDIX A

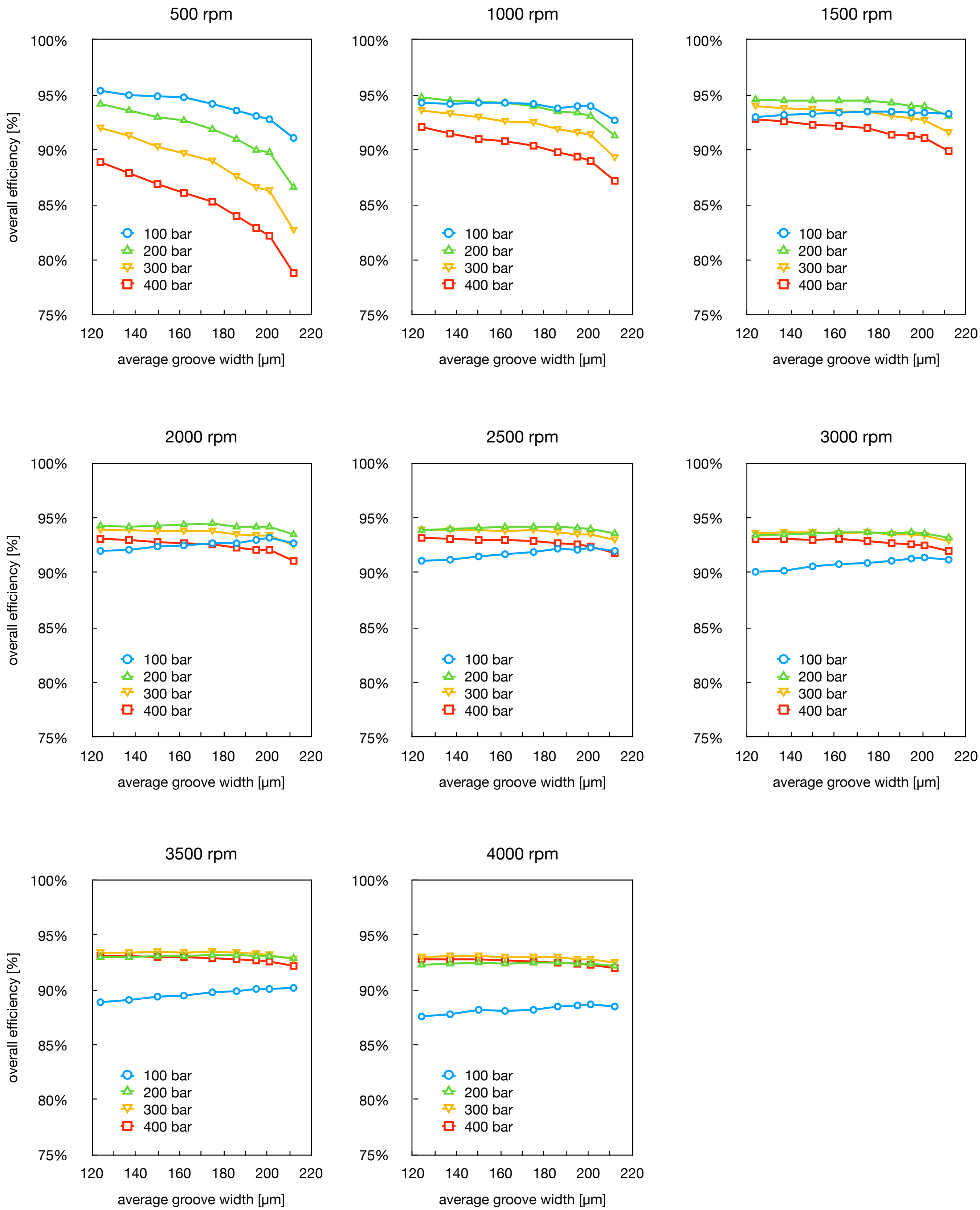

Fig. A.1: Effect of the average groove width on the overall efficiency, for various rotational pump speeds and pressure levels

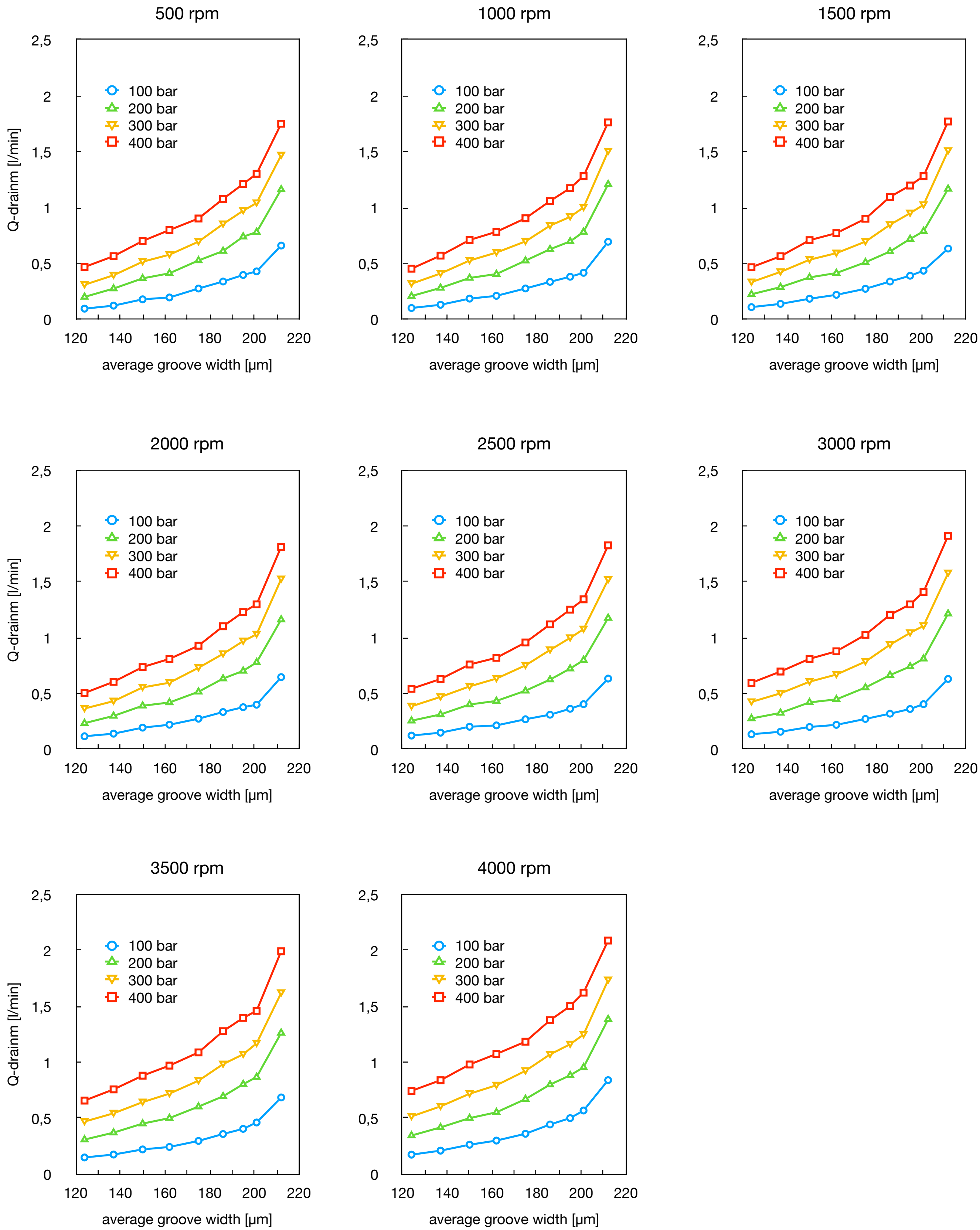

Fig. A.2: Effect of the average groove width on the measured drain flow, for various rotational pump speeds and pressure levels

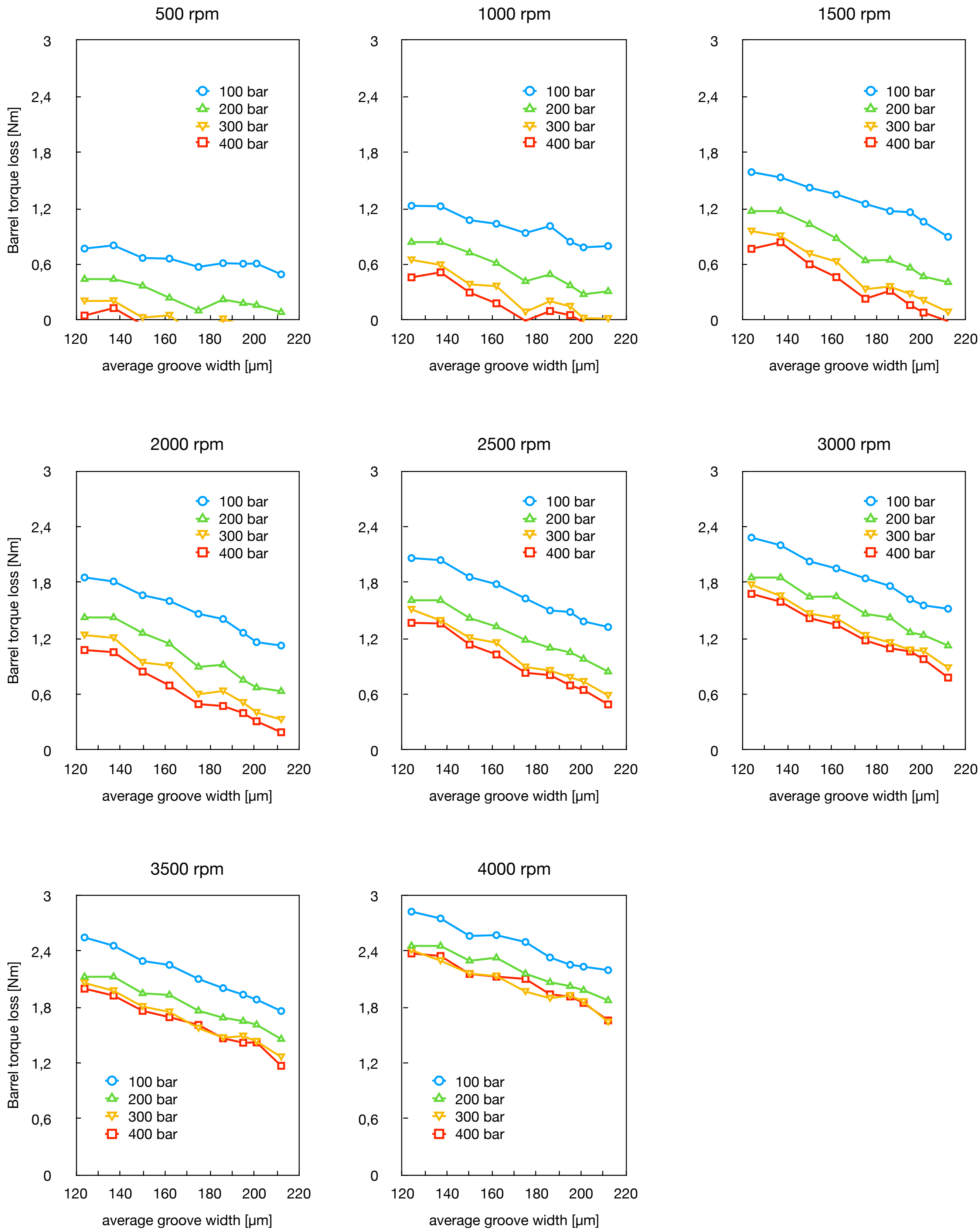

Fig. A.3: Effect of the average groove width on the friction of the barrels (barrel torque loss), for various rotational pump speeds and pressure levels